Sensors and Materials, Vol. 34, No. 6 (2022) 2467–2478
MYU Tokyo

S & M 2983

Integration of Second-generation On-board Diagnostics Data via Deep Learning to Develop Eco-driving Analysis System Applicable to Large and Small Cars

Chi-Chun Chen,[1] Shang-Lin Tian,[1] Chung-Chen Teng,[1]
Cheng-Wei Yang,[2] and Meng-Hua Yen[1*]

[1]Department of Electronic Engineering, National Chin-Yi University of Technology, Taichung 41170, Taiwan
[2]CANDOMO Technology Corporation Limited, Taichung 423, Taiwan

(Received December 31, 2021; accepted June 6, 2022)

Keywords: eco-driving, fuel consumption, second-generation on-board diagnostics (OBD-II), driver behavior analysis

Reducing greenhouse gas emissions is an imperative of climate policy worldwide. The transport sector accounts for a large proportion of CO_2 emissions; therefore, the development of eco-driving has become a critical topic in the study of fuel efficiency and environmental protection. Although considerable research has been carried out on cars, there has been little research involving large vehicles. In this study, second-generation on-board diagnostics (OBD-II) was used to sense and collect the driving data of cars and light-duty buses. These data were then used for predicting real-time fuel consumption by using deep learning methods and a fuel efficiency driving analysis system for both large and small cars. The prediction results demonstrated a correlation coefficient of approximately 90% with actual data and confirmed the applicability of the system to different vehicle types. This system can be integrated with professional driver training centers to improve training quality and promote the development of eco-driving.

1. Introduction

The reduction of atmospheric greenhouse gases is a major goal of international climate policies. The 2015 United Nations Framework Convention on Climate Change achieved a milestone with the Paris Agreement, a framework for lowering Europe's greenhouse gas emissions by 32% by 2030.(1) The transport sector accounts for nearly a quarter of global CO_2 emissions (21–25%).(2) Statistics by Taiwan's transportation department in 2019 indicated that a single large vehicle emitted, on average, approximately 43.4 metric tons of CO_2 in that year, considerably higher than the 2.5 metric tons emitted by single small cars, and that the total emissions of large vehicles comprised approximately 25% of total CO_2 emissions in the transport sector.(3) These numbers demonstrate that commercial large vehicles still account for a considerable proportion of emissions in the transport sector. A recent trend is eco-driving,(4) a

*Corresponding author: e-mail: emh1989@ncut.edu.tw
https://doi.org/10.18494/SAM3796

ISSN 0914-4935
https://myukk.org/

method of driving that minimizes environmental impact. Eco-driving can effectively reduce greenhouse gas emissions by approximately 30%[5] and fuel consumption by 10–15%.[6–11]

Sanguinetti *et al.* proposed six aspects of eco-driving: driving, cabin comfort, trip planning, load management, fueling, and maintenance.[12] They pointed out that gentle driving, speed control, the use of heat dissipation and air conditioning, and the choice of route affect fuel consumption. Accordingly, to achieve eco-driving, the factors that affect fuel consumption must first be determined. To decrease fuel consumption, drivers should avoid excessive changes in acceleration and deceleration and minimize their frequency of gear changes.[11,13–16] On the basis of driving parameters such as car speed and engine rotational speed, Jachimczyk *et al.* categorized different driving styles as ordinary, calm, aggressive, and unnatural. They determined that aggressive and unnatural driving greatly increase both fuel consumption and accident rates.[17]

Current research on eco-driving, in addition to raising awareness of fuel-efficient driving,[18] has mostly involved the development of software and hardware devices to assist driving. These typically involve the use of on-board diagnostics (OBD) to sense and export data from the electronic control unit (ECU) to a backend database for analysis. For instance, Yao *et al.* analyzed the external factors affecting fuel consumption and safety by using driving data collected from taxi drivers and calculated a safety index that considered speed and longitudinal and lateral acceleration. They improved the evaluation algorithm by adding a vehicle lateral control index.[19] Magana and Munoz-Organero proposed the use of genetic algorithms, fuzzy logic, and clustering algorithms to analyze fuel consumption among small cars and used gamification to encourage eco-driving by drivers; their results demonstrated an average 11% decrease in fuel consumption.[6] Meseguer *et al.* used second-generation OBD (OBD-II) to collect speed, acceleration rate, engine rotational speed, mass flow, manifold absolute pressure, and intake air temperature to determine driving styles and route types and demonstrate the relationship between behavior and fuel consumption, which can be used to decrease fuel consumption and greenhouse gas emissions.[5] Jiménez-Palacios proposed the concept of vehicle-specific power to calculate the fuel consumption and greenhouse gas emissions of vehicles. Their model considers air resistance, acceleration rate, rolling resistance, slope, and vehicle load on the basis of kinetic and potential energy.[20] As can be seen from these studies, using vehicle data to promote eco-driving is the current mainstream in research.

Research on the use of artificial neural networks (ANNs) in cars to assist eco-driving has also become popular. However, research on ANNs and eco-driving in large vehicles is less common. Furthermore, there has been no research involving models that predict the fuel consumption of both large and small cars. In this study, we developed an ANN model based on the OBD-II system that can predict the fuel consumption of both large and small cars.

2. Materials and Methods

2.1 System and hardware devices

Figure 1 shows a schematic of the system developed in this study. An integrated OBD-II module receives the driving data of large and small cars during the driving process, then

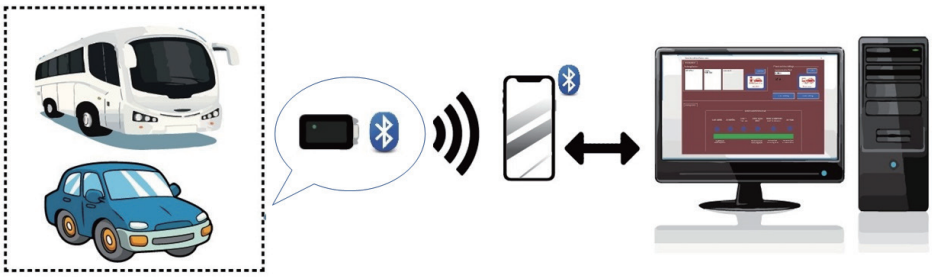

Fig. 1. (Color online) System schematic.

transmits the data via Bluetooth to a smartphone. The data are then relayed to the backend database, which stores the driving data. The data are subsequently used in deep learning to analyze and predict fuel consumption.

Figure 2 depicts the OBD-II module, which was built using a PIC18F46K80 microprocessor. To ensure that the system can be adapted to multiple car models and communicate with large and small cars, the OBD-II module was integrated with the CAN BUS protocol. The vehicle's driving data are transmitted via Bluetooth to a phone and computer terminal.

2.2 User interface

Our newly designed graphical user interface (GUI) is presented in Fig. 3. The upper half is the settings zone, and the lower half is the display zone. Block 1 allows the selection of the driver and vehicle. Block 2 allows the selection of the COM port connection; if the connection is normal, the icon will change from blue to green. Block 3 displays six types of inefficient behaviors: excessive vehicle speed, excessive rotational speed, excessive idling, too low gear, rapid acceleration or deceleration, and use of air brakes. If an inefficient behavior is detected, the signal turns red. We also integrated multiple vehicle parameters with deep learning to determine real-time fuel consumption during driving, which is displayed as a bar gauge to alert the driver of excessive fuel consumption.

2.3 Experimental routes

The purpose of the study was to verify the accuracy of the system's fuel consumption predictions for different vehicle models and routes. The test cars were cars and a light-duty bus. The two test routes both included flat roads and mountain roads (Fig. 4). The car route was used when testing the system during its initial development and was 12.3 km in length, consisting of 3.9 km of flat roads and 8.4 km of inclined mountain roads. The bus route was the test route used by the Central Region Training Center of the Directorate General of Highways, R.O.C., to train professional drivers applying for class II large passenger vehicle licenses; the route was 11.8 km long and comprised 2 km of flat roads and 9.8 km of gentle mountain roads.

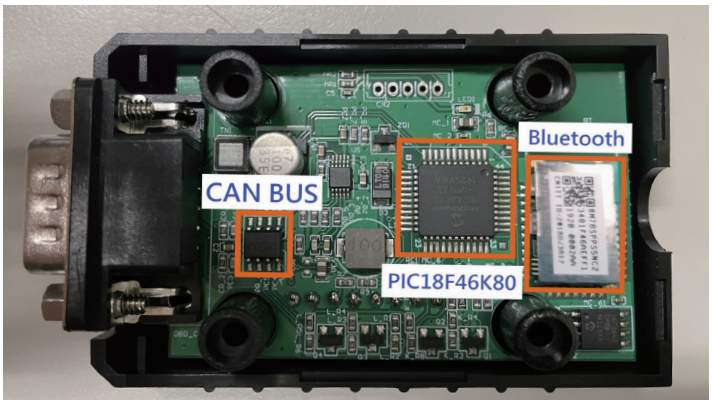

Fig. 2. (Color online) OBD-II module.

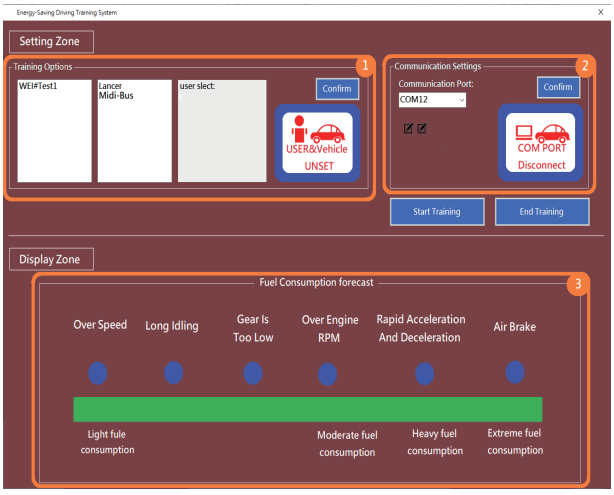

Fig. 3. (Color online) GUI.

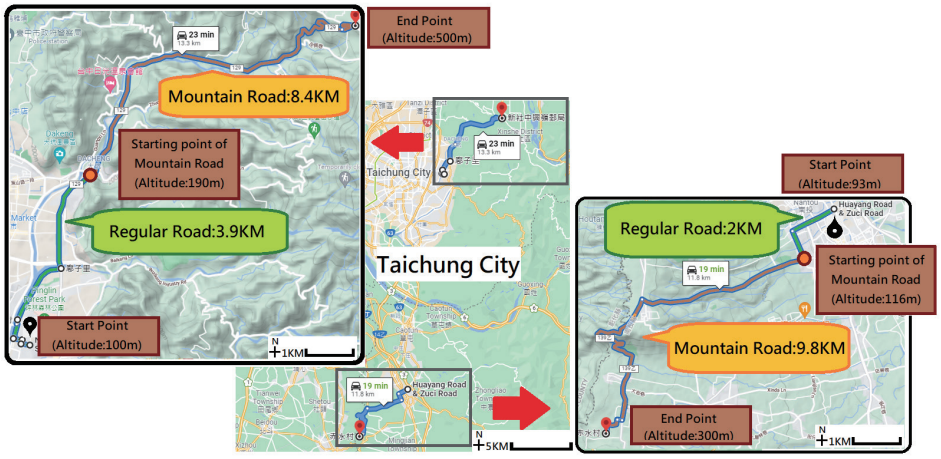

Fig. 4. (Color online) Driving routes.

2.4 Data collection and preprocessing

Table 1 presents the data collected in this study, which included data from three cars and one bus. The data from these four vehicles were used as the training data for the ANN; subsequently, one car and the bus were selected to produce the testing data. The driving parameters were variables that influenced fuel consumption or reflected driving conditions (Table 2). The seven identified variables were engine displacement, engine coolant temperature, engine load, engine rotational speed, weight of rotation, vehicle speed, and throttle position.

In this study, fuel consumption was calculated as

$$Fuel\,Consump_{inst} = \frac{RPM\,Weight_{avg} \times EL_{avg} \times 2.3 \times Fuel\,Factor \times t \times ED}{7545}, \tag{1}$$

where $RPMWeight_{avg}$ and $FuelFactor$ were defined numerically in our previous work.[21] EL_{avg} is the OBD output of the engine load, ED is the vehicle's rated engine displacement in cubic centimeters, and t is the duration of fuel consumption calculated in seconds.

The data must undergo preprocessing, which involves normalization to standardize the scales of different input parameters, before it is input into the ANN model for training. The formula used for normalization was

$$N = \frac{n - I_{min}}{I_{max} - I_{min}}, \tag{2}$$

where N is the normalized value, n is the prenormalized value, and I_{min} and I_{max} are the minimum and maximum values of the parameter, respectively.

Table 1
Vehicle models used in experiment.

Brand	Module	Base curb weight (kg)	Engine torque	Engine displacement (c.c.)	Fuel factor
Toyota	COASTER	5400	40.5 kg·m/1800 rpm	4009	1
Mazda	Mazda 3	1370	21.7 kg·m/4000 rpm	1999	0.87
Mitsubishi	Lancer 1.8	1400	17.9 kg·m/4200 rpm	1798	1.17
Toyota	Vios	1080	14.3 kg·m/4200 rpm	1496	1.48

Table 2
ANN input parameters.

Parameter	Unit	Range of parameter
Engine displacement	c. c.	0–16384
Engine coolant temperature	℃	−40–215
Engine load	%	0–100
Engine rotational speed	RPM	0–16384
Weight of rotation		2–100
Vehicle speed	km/h	0–255
Throttle position	%	0–100

2.5 ANN models and processing procedures

An ANN-based vehicle data model was proposed in this study. Neural networks (NNs) have already been widely used to establish complex relationships between inputs and outputs. The three models used in this study were the feed-forward backprop (FFB), Elman backprop, and layer recurrent (LR) models. Elman NNs[21] and LRNNs[22] are recurrent NN (RNN) structures. RNNs have a context layer that can treat the current status as the input of the next unit time; consequently, continuous information changes are recorded in the network, improving prediction accuracy. The model framework is depicted in Fig. 5. The main RNN equation is expressed as

$$s_i(t) = g\left\{\left(\sum_{m=1}^{M} v_{im} s_m(t-1) + \sum_{m=1}^{M} w_{in} I_n(t-1)\right)\right\}, \tag{3}$$

where $s_m(t-1)$ is the status output of the previous unit time, $I_i(t)$ is the input, v_{im} and w_{in} are their respective weights, and g is the sigmoid function.

The activation function is a nonlinear function, which is defined by specifying its range according to the NN weighted value, then repeatedly superimposing the range until the NN can obtain the data characteristics. In this study, the following logistic sigmoid function was used:

$$g = \frac{e^{x} - e^{-x}}{e^{x} + e^{-x}}. \tag{4}$$

The model was trained using a PC equipped with an Intel Xeon Gold 5220R (2.20 GHz) CPU, a Microsoft Windows 10 for Business operating system, 16 GB RAM, and a graphics card with a normal module (NVIDIA, RTX-2080Ti 8 GB). The analysis software used was MATLAB (MathWorks, Inc., Natick, MA, USA). To ensure that the models could be compared, the models were configured using the same numbers of layers and neurons. The training function was TRAINLM, and the activation function was TANSIG, which is the aforementioned sigmoid function. The final step was to validate the prediction results by using three indicators commonly

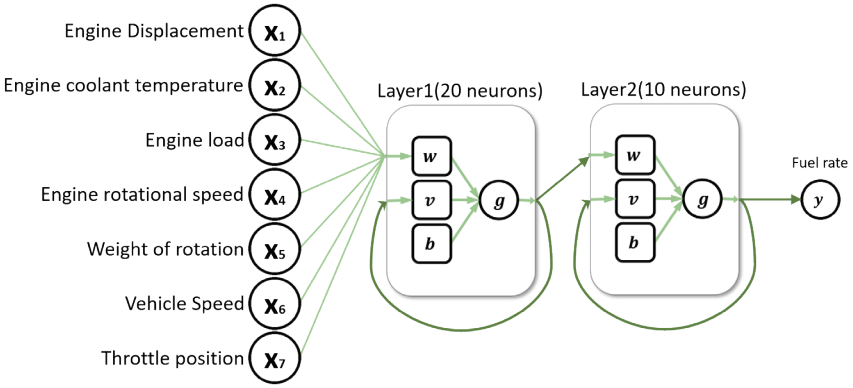

Fig. 5. (Color online) Recurrent NN.

used to evaluate model effectiveness: root mean squared error (RMSE), normalized root mean square error (NRMSE), and the correlation coefficient (γ):

$$RMSE = \sqrt{\frac{1}{n}\sum_{i=1}^{n}\left(y_i - \hat{y}_i\right)^2}, \tag{5}$$

$$NRMSE = \frac{RMSE}{y_{i_{max}} - y_{i_{min}}}, \tag{6}$$

$$\gamma = \frac{\sum_{i=1}^{N}\left(\hat{y}_i - \overline{\hat{y}_i}\right)\left(y_i - \overline{\hat{y}_i}\right)}{\sqrt{\sum_{i=1}^{N}\left(\hat{y}_i - \overline{\hat{y}_i}\right)^2} * \sqrt{\sum_{i=1}^{N}(y_i - \overline{\hat{y}_i})^2}}. \tag{7}$$

Here, n is the data length, y_i is the raw data, and $\hat{y}_i$ is the outcome of the NN prediction.

3. Results

Figure 6 depicts line graphs of predicted instantaneous fuel consumption versus driving time. As shown in Fig. 6(a), as the car drove along flat roads (approximately 0 to 950 s), the FFB line (orange) exhibited the greatest error and the LR line exhibited the second greatest error. As the car traveled along the mountain roads (950 to 1600 s), the FFB had a lower prediction accuracy than the other two models; during the frequent accelerations and decelerations on mountain roads, FFB was prone to overestimation in its predictions. The discrepancies between the two RNNs were small. These traits are reflected in Table 3.

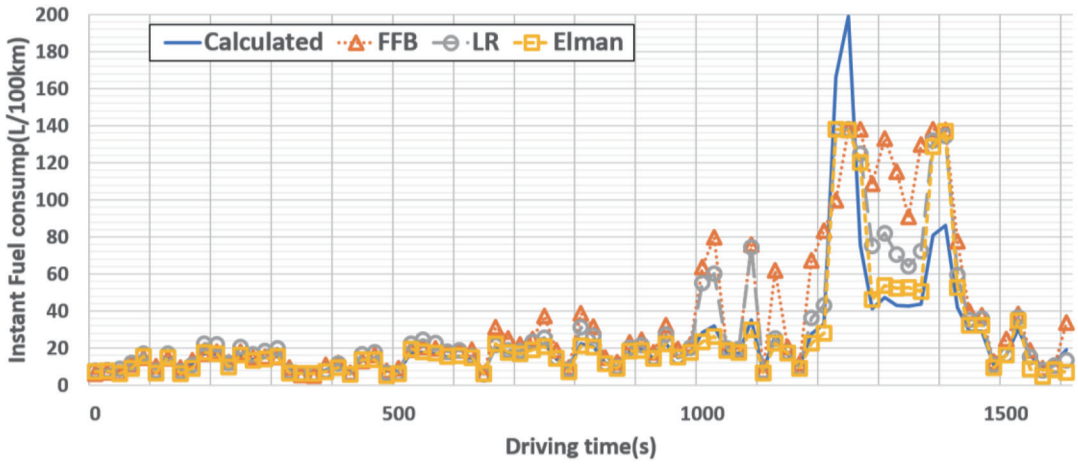

(a)

Fig. 6. (Color online) Calculated instantaneous fuel consumption (blue) versus FFB model (orange), Elman NN (yellow), and layer NN model (grey) predictions: (a) Mitsubishi car and (b) Toyota light-duty bus.

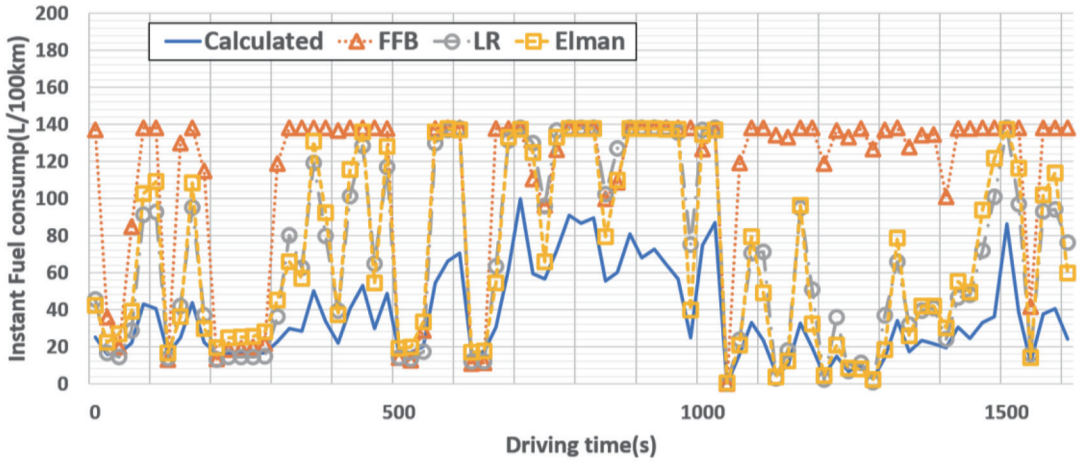

(b)

Fig. 6. (Continued) (Color online) Calculated instantaneous fuel consumption (blue) versus FFB model (orange), Elman NN (yellow), and layer NN model (grey) predictions: (a) Mitsubishi car and (b) Toyota light-duty bus.

Table 3
Comparison of predictions of vehicle fuel consumption for previous system[21] and two RNN models.

Vehicle type	Lancer[21]			Lancer			COASTER		
NN model	FFB	LR	Elman	FFB	LR	Elman	FFB	LR	Elman
RMSE	9.742	6.637	4.077	22.182	12.401	10.754	85.427	42.767	44.449
NRMSE		N/A		0.167	0.092	0.08	0.619	0.31	0.324
γ	0.793	0.977	0.97	0.753	0.897	0.91	0.427	0.931	0.911

As shown in Fig. 6(b), as the bus traveled along flat roads (approximately 0 to 300 s), the three models exhibited greater errors than those for the car but maintained a certain level of correlation. Among the three models, the Elman model showed the best performance. The fuel consumption was greater while traveling along the mountain roads (approximately 350 to 1050 s and after 1450 s), and the two RNN models were clearly more capable than FFB in keeping up with the changes in fuel consumption. Fuel consumption was lower during and after the downhill portion of the mountain roads (approximately 1050 to 1450 s) due to frequent braking, and the two RNN models also demonstrated more accurate correlations than FFB in this period. FFB also showed greater errors in fuel consumption prediction than the other models during uphill driving.

In this study, the prediction error for cars was greater than that in prior research,[21] mainly because the bus we used did not contain ECUs such as for the battery voltage or ignition timing. The different training datasets may have also reduced the fuel consumption predictions for small cars. Furthermore, to facilitate comparisons between large and small cars, the number of input parameters was reduced (Table 2). According to our result, the Mitsubishi Lancer had relatively high correlations (data not shown); therefore, it was used as the small car for comparison with the bus.

According to Table 3, among the three models, the Elman model displayed the smallest errors in its predictions for cars; its RMSE was 10.7542, its NRMSE was 0.0804, and its γ was 91.01%. The LR model had the second-best performance, with an RMSE of 12.4008, an NRMSE of 0.0917, and γ of 89.71%. The worst-performing model was FFB, with an RMSE of 22.1815, an NRMSE of 0.1669, and γ of 75.33%. Although the car parameters were less favorable than those in other studies, the results displayed similar trends to those in other studies, and the two RNN models exhibited robust prediction performance, with the best performance from the Elman model. Among the bus results, the FFB model had the worst performance of the three models, with an RMSE of 85.4273, an NRMSE of 0.619, and γ of 42.73%. The other two RNN models had similar RMSE values (Elman = 44.4489; LR = 42.7666) and correlations (Elman: γ = 91.1%; LR: γ = 93.1%). Consequently, applying the two RNN models improved the performance of the fuel consumption predictions.

Figure 7 shows an image of the bus on the road. If the driver neglects to change gears, resulting in an overly high rotational speed and overly low power output, the GUI signals turn from blue to red. This immediately alerts the driver that their driving style is inefficient. Simultaneous deep learning calculations convert the instantaneous fuel consumption to a bar gauge that enables the driver to improve their driving behaviors.

4. Discussion

The goal of this study was to promote the application of eco-driving assistance systems to more vehicle types on the basis of previously developed general-purpose OBD-II systems. Driving data from cars and a bus on two different routes were used as ANN training datasets for predicting and analyzing fuel consumption for different car and route types. Fuel consumption predictions involving different vehicle models and routes demonstrated strong correlations with actual fuel consumption, with a correlation coefficient as high as 90%. The results indicate that the system proposed in this study is applicable to both large and small cars and can obtain robust fuel consumption predictions for both vehicle types. In the future, this system can be applied to larger vehicles.

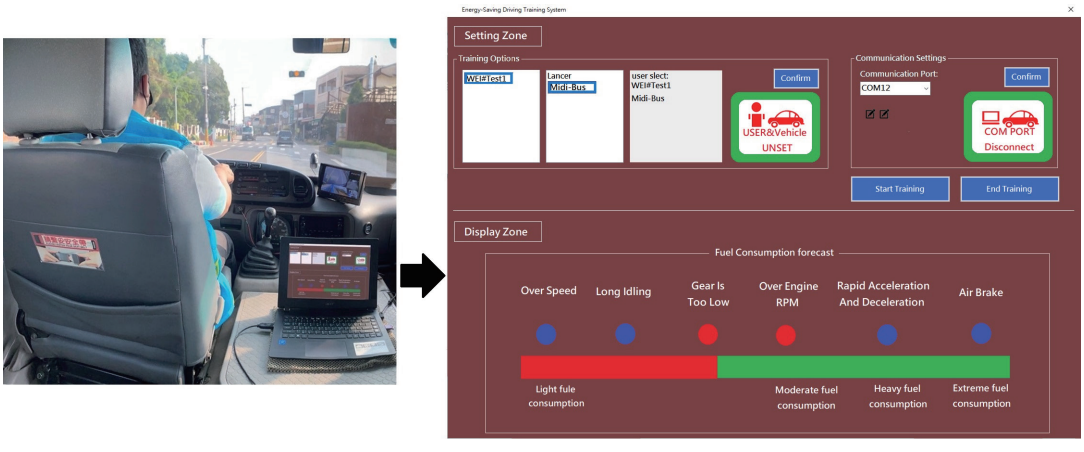

Fig. 7. (Color online) Actual driving image and GUI.

As depicted in Fig. 6, for both vehicle types, better results were obtained with the RNN models (i.e., the Elman model and LR model) than with the FFB model. These results are similar to the car fuel consumption predictions in a previous study,[12] indicating that RNN models are more suitable for the prediction and analysis of fuel consumption. The bus fuel consumption predictions in this study were similar to those of Xu *et al*.,[23] who found that frequent acceleration and deceleration was the main cause of increased fuel consumption and also reduced the performance of fuel consumption prediction. Conversely, in this study, driving at lower and more stable engine speeds led to lower error values in fuel consumption predictions, as can be seen in Fig. 6. Although the FFB predictions for buses were considerably inferior to those for cars, the FFB is a critical basic NN model and therefore a major reference model for comparison. We plan to test and validate our proposed system by using more vehicle types (such as large passenger cars and trailers) to improve the performance of fuel consumption prediction and to analyze and broaden the application scope of the system.

According to the outcomes illustrated in Fig. 6, while driving on mountain roads, the car and bus demonstrated visible discrepancies in their fuel consumption changes [950–1600 s in Fig. 6(a) and from 350 s in Fig. 6(b)]. A possible reason may be differences in the slope between the two routes along the mountain roads. The car gained 37 m altitude per kilometer along the mountain roads, whereas the bus gained 19.3 m altitude per kilometer (Fig. 4). Furthermore, the bus has a greater load-bearing capacity and can be expected to demonstrate smaller changes in engine load than a car, even on mountain roads with similar slopes. Therefore, different cars will exhibit different changes in fuel consumption under the effects of different slopes. In the future, a gyroscope sensor can be added to detect the slope and achieve more accurate fuel consumption prediction.

The bus route used in this study was the training route used to train professional drivers by the Central Region Training Center of the Directorate General of Highways, R.O.C. The proposed system can be used at the training center to facilitate the acquisition of eco-driving behaviors in professional drivers. It can also produce reports for students and coaches to assess learning progress.

5. Conclusions

The collection of driving data is essential to the development of eco-driving and vehicle safety. In this study, OBD-II was used to sense and collect real-time driving data from cars and a light-duty bus. The data were then used in deep learning systems for predicting real-time fuel consumption and in an energy-saving driving analysis system for both large and small cars. Among the three ANN models used in this study, the RNN (i.e., Elman and LR) predictions demonstrated correlation coefficients of approximately 90% with the actual data. The results verified the applicability and feasibility of the system to different vehicle types. The system can be used to assist professional driver training in the future and advance the development of eco-driving.

Author Contributions

Conceptualization, C.-C.C. and M.-H.Y.; methodology, C.-C.C., M.-H.Y., S.-L.T., and C.-C.T.; software, S.-L.T., C.-C.T., and C.-W.Y.; validation, S.-L.T., C.-C.T., and C.-W.Y.; formal analysis, S.-L.T. and C.-C.T.; investigation, C.-C.C. and M.-H.Y.; resources, C.-C.C. and C.-W.Y.; data curation, C.-C.C. and C.-W.Y.; preparation of original draft, C.-C.C. and M.-H.Y.; review and editing, C.-C.C. and M.-H.Y.; visualization, C.-C.T. and C.-W.Y.; supervision, C.-C.C. and M.-H.Y.; project administration, C.-C.C. and M.-H.Y.; funding acquisition, C.-C.C. and M.-H.Y. All authors have read and agreed to the published version of the manuscript.

Funding

This research was funded by the Ministry of Science and Technology, Taiwan (grant numbers MOST 109–2622–E-167–022–, MOST 110–2622–E-167–017, and MOST 111–2622–E–167–002–).

Acknowledgments

The authors would like to thank the Automotive Research and Testing Center (ARTC), Changhua, Taiwan, for their valuable assistance in the vehicle experiments.

Conflicts of Interest

The authors declare no conflict of interest.

References

1 The United Nations Framework Convention on Climate Change (UNFCCC): https://unfccc.int/files/essential_background/convention/application/pdf/english_paris_agreement.pdf (Accessed October 2021)
2 Iea Institution, https://www.iea.org/data-and-statistics/data-browser?country=WORLD&fuel=CO2%20emissions&indicator=CO2BySector (Accessed October 2021)
3 Institute of Transportation, Motc, https://data.gov.tw/en/datasets/8331 (Accessed October 2021)
4 R. C. McIlroy and N. A. Stanton: Ergonomics **60** (2017) 754. https://doi.org/10.1080/00140139.2016.1227092
5 J. E. Meseguer, C. K. Toh, C. T. Calafate, J. C. Cano, and P. Manzoni: J Commun. Networks **19** (2017) 162. https://doi.org/10.1109/jcn.2017.000025
6 V. C. Magana and M. Munoz-Organero: IEEE Trans. Mob. Comput. **15** (2016) 2437. https://doi.org/10.1109/tmc.2015.2504976
7 C. Rolim, P. Baptista, G. Duarte, T. Farias, and J. Pereira: IEEE Trans. Intell. Transp. Syst. **18** (2017) 3061. https://doi.org/10.1109/tits.2017.2657333
8 K. Ayyildiz, F. Cavallaro, S. Nocera, and R. Willenbrock: Transp. Res. F: Traffic Psychol. Behav. **46** (2017) 96. https://doi.org/10.1016/j.trf.2017.01.006
9 O. Mata-Carballeira, M. Diaz-Rodriguez, I. del Campo, and V. Martinez: Appl. Sci. (Basel) **10** (2020). https://doi.org/10.3390/app10186549
10 D. Lois, Y. Wang, A. Boggio-Marzet, and A. Monzon: Transp. Res. D: Transp. Environ. **72** (2019) 232. https://doi.org/10.1016/j.trd.2019.05.001
11 A. Zavalko: Transp. Res. D: Transp. Environ. **62** (2018) 672. https://doi.org/10.1016/j.trd.2018.01.023
12 A. Sanguinetti, K. Kurani, and J. Davies: Transp. Res. D: Transp. Environ. **52** (2017) 73. https://doi.org/10.1016/j.trd.2017.02.005
13 P. Ping, W. H. Qin, Y. Xu, C. Miyajima, and K. Takeda: IEEE Access **7** (2019) 78515. http://dx.doi.org/10.1109/access.2019.2920489

14 J. Diaz-Ramirez, N. Giraldo-Peralta, D. Florez-Ceron, V. Rangel, C. Mejia-Argueta, J. I. Huertas, and M. Bernal: Transp. Res. D: Transp. Environ. **56** (2017) 258. https://doi.org/10.1016/j.trd.2017.08.012
15 E. Ericsson: Transp. Res. D: Transp. Environ. **6** (2001) 325. https://doi.org/10.1016/s1361-9209(01)00003-7
16 N. Robuschi, M. Salazar, N. Viscera, F. Braghin, and C. H. Onder: IEEE Trans. Veh. Technol. **69** (2020) 14575. https://doi.org/10.1109/tvt.2020.3030088
17 B. Jachimczyk, D. Dziak, J. Czapla, P. Damps, and W. J. Kulesza: Sensors **18** (2018). https://doi.org/10.3390/s18041233
18 D. Baric, G. Zovak, and M. Perisa: Promet-Traffic & Transportation **25** (2013) 265. https://doi.org/10.7307/ptt.v25i3.1260
19 Y. Yao, X. H. Zhao, Y. L. Zhang, C. Chen, and J. Rong: Transp. Res. D: Transp. Environ. **79** (2020) 102224. https://doi.org/10.1016/j.trd.2020.102224
20 J. L. Jimenez-Palacios: Thesis (Ph.D.), Massachusetts Institute of Technology (1999). https://dspace.mit.edu/handle/1721.1/44505
21 M. H. Yen, S. L. Tian, Y. T. Lin, C. W. Yang, and C. C. Chen: Appl. Sci. (Basel) **11** (2021). https://doi.org/10.3390/app11104481
22 J. L. Elman: Cogn. Sci. **14** (1990) 179. https://doi.org/10.1207/s15516709cog1402_1
23 Z. G. Xu, T. Wei, S. Easa, X. M. Zhao, and X. B. Qu: Comput.-Aided Civ. Infrastruct. Eng. **33** (2018) 209. https://doi.org/10.1111/mice.12344